

New broken-parity state and a transition to anomalous lamellae in eutectic growth

Klaus Kassner

Institut für Festkörperforschung des Forschungszentrums Jülich, W-517 Jülich, Germany

Alexandre Valance,* Chaouqi Misbah, and Dmitrii Temkin[†]

Institut Laue Langevin, Boîte Postale 156X, 38042 Grenoble CEDEX, France

(Received 12 January 1993)

We discover that a eutectic system exhibits pseudobcritical features corresponding to the simultaneous birth of two different broken-parity states. The first branch is the known tilted-growth mode, i.e., *global parity breaking*; it bifurcates from the usual lamellar symmetric state. At approximately the same critical point, a second branch merges close to the second *fold* we found previously. The two states thus bifurcate from different basic states. This new branch owes its existence to the underlying degeneracy of the usual broken-parity state. It consists of a structure where one lamella assumes a right-traveling and the other a left-traveling state. As a consequence, the drift velocity (or equivalently the tilt angle) is smaller for the new branch. Close to the bicritical point, the bifurcation is described by a Landau theory with the tilt angle being the order parameter. From general considerations we can state that the new branch is locally stable in the kinetic sense, but less stable than the usual branch. This result is consistent with the conventional criterion based on comparison of undercooling, since the new branch has a higher undercooling. We propose a simple experimental protocol to have access to the new state. Finally, when the two lamellae have equivalent properties (a symmetric case) the new state is not traveling while each lamella is asymmetric with respect to its center and is a mirror image of the other lamella. This corresponds to the so-called anomalous cells observed in noneutectic systems. We develop an analytic theory, in the same spirit as the one used for the parity breaking, to account for the transition to the anomalous state. The results are in qualitative agreement with the full numerical calculation.

PACS number(s): 61.50.Cj, 05.70.Fh, 81.30.Fb, 68.70.+w

I. INTRODUCTION

It is well known that directional solidification of normal binary eutectic systems typically gives rise to lamellar or fibrous structures. Since considerable progress has been made in the problem of eutectic growth during the past few years, we briefly recall the main lines of research and the current state of affairs. In 1966, Jackson and Hunt (JH) gave a theoretical description of eutectic structures that has remained a standard reference until today [1]. They simplified the problem to render it analytically tractable by replacing the diffusion field in the liquid phase with that of a planar front. Furthermore, they assumed that the lamellae of the two phases have equal average undercoolings, which allows the derivation of an analytic expression for the average undercooling. As a function of the wavelength, it exhibits a minimum.

It was then tempting to conjecture that the wavelength associated with this minimum is *selected* in lamellar growth. As a heuristic criterion, this hypothesis had been originally proposed by Zener [2]. Cahn was the first to point out that a eutectic structure with a wavelength smaller than the one predicted by this criterion would be inherently unstable, and the argument was explained in some detail by JH [1]. Experimentally, the dispersion of wavelengths *in a single eutectic grain* is small, so a selection mechanism might indeed be operative.

Theoretical work following the Jackson-Hunt calculation first focused on improving the accuracy of the

description. Nash [3] developed a boundary-integral formulation for the problem but had to introduce various approximations to make it tractable. Series, Hunt, and Jackson [4] approached the moving-boundary problem via construction of an electrostatic analogue made of resistance paper (with cuts defining the interface shape). They determined interface shapes in the limit of vanishing Péclet number. Their calculations already hinted at the fact that symmetric solutions do not exist for arbitrarily large wavelengths.

Trivedi, Magnin, and Kurz [5] extended the work of JH to the limit of large Péclet numbers (rapid solidification) and discussed the behavior of the minimum undercooling as a function of velocity. They still assumed local thermal equilibrium at high pulling speeds. On the other hand, a kinetic term had even earlier been included into the description of the interface undercooling for *isothermal* eutectic growth [6,7].

In these analytic approaches the flat interface and equal undercooling assumptions of JH were used [4–7]. Brattkus *et al.* [8] recently suggested that the former assumption is justified only for large thermal gradients, that is, when $l_T/l \ll 1$, where l is the diffusion length and l_T a thermal length. It turned out from our full calculation, however, that the JH approximation is valid (in the vicinity of the minimum undercooling) even for $l_T \sim l$. Careful inspection of the equations [9] shows that the appropriate expansion parameter is λ/l_T , which is always small, and not l_T/l as in Ref. [8]. If one uses huge thermal gradients

(10^3 bigger than standard ones), values of order one of the parameter λ/l_T can be reached and the isothermal assumption ceases to be valid. Besides academic cases ($l_T \sim \lambda$) we can ascertain now that the JH theory describes remarkably well the symmetric pattern if λ is not too far from the wavelength that provides the minimum undercooling (but it misses other important features; see below).

A fundamental question was addressed by Langer [10] and by Datye and Langer [11], who tried to justify the minimum undercooling criterion by a stability calculation, identifying it as the point of marginal stability of the system. A more recent analysis [12] concludes that a simplifying assumption used in their calculation is unjustified in the limit of large thermal gradients, where the point of minimal undercooling turns out to be stable. In view of the remark made above, this is not surprising, since in this limit the very large value of the thermal gradient also invalidates the isothermal assumption assumed by Langer [10]. We can state, as for the JH theory, that Langer's [10] result should describe well phase instability as long as $l_T \gg \lambda$, a situation which is always met in experiments. It is, however, important in order to obtain conclusive answers about the general case to perform a full treatment of diffusive instabilities [13] at an arbitrary thermal gradient, along the lines of similar work on directional solidification of dilute alloys [14].

Also worth mentioning is a numerical simulation of the eutectic system by Karma [15]. It was based on a random-walker model and gave the first *theoretical* evidence for a tilting instability. Karma did not, however, investigate the nature of the bifurcation nor did he obtain quantitative results for the tilt angle as a function of system parameters. This is quite difficult with his inherently noisy method.

Interest in the growth of eutectic systems has been revived by experiments [16] and by our recent work [17–23]. The experiment in question demonstrated unambiguously that *parity-breaking* structures similar to those seen in an earlier experiment on liquid crystals [24] do exist in the eutectic system (a fact that actually has been known to metallurgists for some 20 years at least [25]). With regard to parity breaking in general, the phenomenology of Coulet, Goldstein, and Gunaratne [26] has constituted a crucial step.

Our research explained the nature of parity breaking (which is the consequence of a *supercritical* bifurcation) and led to the suggestion of new experiments to clarify this nature [17,20,21], one of which has actually been successfully performed meanwhile [27]. Furthermore, it revealed features that go essentially beyond the Jackson-Hunt theory [18,19,21], such as the existence of a discrete set of axisymmetric solutions for a given parameter set, the existence of a fold singularity in the bifurcation diagram at which symmetric solutions cease to exist, or a novel scaling relation for the selected wavelength both in untilted and tilted eutectic growth. Follow-up work included a numerical confirmation of this scaling relation for an improved JH-type theory [28], an explanation of *localized* tilted domains via the coupling between parity breaking and the phase of the pattern [29], which we ex-

tended to the case of anisotropic surface tension [30]. A *dynamical wavelength selection mechanism*, suggested by Coulet, Goldstein, and Gunaratne [26], has meanwhile also been found in experiments [31].

Another recent development pertains to an analytic treatment for parity breaking. Except in the situation where one can model the front dynamics by a two-mode coupling [32,33]—a situation which holds close to a codimension-two bifurcation of the planar interface—all the knowledge on parity breaking came from numerical calculations. In particular, the eutectic system (which cannot be modeled by two resonant Fourier modes) seemed to defy an analytic treatment. Recently, we have been able [22,23] to develop a successful analytic theory for the parity-breaking bifurcation which captures the essential physical features, plus some new developments.

We now turn to the main purpose of the present contribution. In one of our previous investigations [20], we speculated that there should exist another broken-parity traveling state in addition to the one we discovered previously. Meanwhile, we have indeed found a new branch which merges—within numerical uncertainties—at the same critical point. Let us recall that the old branch corresponds to a profile structure where each lamella assumes the same sign for the antisymmetric part (both lamellae types would travel in the same direction if each of those types were alone). Since parity breaking is a pitchfork bifurcation, there exists a degeneracy corresponding to the fact that right- and left-traveling states are physically equivalent. Due to this degeneracy, there is in the present case another degree of freedom leading to a physically different state. Indeed, one can imagine that each lamella would, somehow, maintain its identity such that one of them chooses a right-traveling state while the other chooses a left-traveling one. This is what the new solution consists of. Since both lamellae are pointing in opposite directions, the drift velocity of the pattern—or equivalently the tilt angle—is smaller than that of the old solution. The old branch merges close to the lower fold (see later) discovered previously [20], while the new one does so close to the upper fold. In other words the *mother states* for both solutions are different. There is thus no true bi-criticality, and therefore we shall often use the denomination pseudobcriticality. This is taken to mean that both solutions appear at the same critical point (e.g., the same velocity) but their basic states are distinguishable.

Close to the same pseudobcritical point we shall write down a general Landau equation, the tilt angle being the order parameter. We shall see that the new branch is metastable (in the variational formulation that is possible close to criticality). The new branch also has a higher undercooling. Thus both criteria (the conventional undercooling one and the kinetic one based on the Lyapunov function) are in favor of the old branch. We shall argue here that existence of the new state should not, however, be devoid of experimental testability. We propose an experimental protocol to have access to the new branch.

The first part of the numerical investigations of this paper was motivated by some results obtained within a

random-walk model devised by Karma [15]. His work dealt with a situation where the two solid phases have exactly the same properties (we shall use the symmetric system denomination throughout this paper). One of his results was that the tilting instability should exist for off-eutectic compositions only. To the contrary, we find that the eutectic point does not play a special role for parity breaking. This also agrees with our previous analytic work [22]. The second part of the question concerning the symmetric system pertains to the development of the new branch when one goes from an asymmetric system to a symmetric one. From symmetry arguments, the new branch should correspond to a front structure, where each lamella is asymmetric with respect to its center and is a mirror image of the other lamella. This is what we find. It should be mentioned that in this (very special) case, as we shall see, it is hard to speak of a pseudobicritical transition since the critical points of the two branches have a few percent difference. This new structure is reminiscent of the so-called anomalous cells observed in noneutectic systems [34–36]. Following the spirit of our previous analytic treatment [22] for parity breaking, we have constructed an analytic theory to account for the transition to the anomalous state. We find that the analytic treatment captures the essential qualitative features.

This paper is organized as follows. In Sec. II we write down the basic equations and briefly recall the numerical strategy. We then present and discuss “exact” numerical results for the symmetric and asymmetric systems. In Sec. III we describe the pseudobicriticality by means of a Landau theory and suggest an experimental protocol to have access to the new branch. Section IV is devoted to the analytic theory accounting for the transition to the anomalous state. Section V contains a discussion of the results and a general outlook.

II. BASIC EQUATIONS AND NUMERICAL RESULTS

A. Mathematical description

The directional solidification setup used to investigate lamellar eutectics (and other systems) has been described in our earlier work [19]. Essentially, the specimen is pulled at constant speed V between two thermal contacts, moving from the hot to the cold one. A constant temperature gradient G can be established by appropriate experimental conditions. The model equations have also been discussed previously, both for the cases of symmetric [19] and nonsymmetric [20,21] patterns. Therefore, we shall simply recall them in their most useful form without dwelling on details. The diffusion equation for the normalized concentration field u ,

$$u = (c - c_e) / \Delta c, \quad (2.1)$$

is cast into the form of an integral equation:

$$\int_{\Gamma_{sl}} d\Gamma' g(\mathbf{r}, \mathbf{r}') \frac{\partial u}{\partial n'} = \int_{\Gamma_{sl}} d\Gamma' h(\mathbf{r}, \mathbf{r}'; \mathbf{n}') \times [u(\mathbf{r}') - u_\infty]. \quad (2.2)$$

For the definitions of the miscibility gap Δc and the eutectic concentration c_e , see the phase diagram given in Fig. 1. The Green’s function $g(\mathbf{r}, \mathbf{r}')$ of the stationary diffusion equation, in a frame attached to the interface, is given by

$$g(\mathbf{r}, \mathbf{r}') = \frac{1}{2\pi} e^{-(\Delta z + \Delta x \tan\phi)/l} K_0 \left[\frac{\rho}{l \cos\phi} \right], \quad (2.3)$$

where $\Delta x = x - x'$, $\Delta z = z - z'$, $\rho = \sqrt{\Delta x^2 + \Delta z^2}$, and $\mathbf{r} = (x, z)$. K_0 is the modified Bessel function of zeroth order. The tilt angle ϕ appears here because it determines the lateral velocity of the pattern ($V_x = V \tan\phi$). Furthermore,

$$h(\mathbf{r}, \mathbf{r}'; \mathbf{n}') = \frac{1}{2\pi l} e^{-(\Delta z + \Delta x \tan\phi)/l} \times \left[-(n'_z + n'_x \tan\phi) K_0 \left[\frac{\rho}{l \cos\phi} \right] - \frac{\mathbf{n}'(\mathbf{r}' - \mathbf{r})}{\rho \cos\phi} K_1 \left[\frac{\rho}{l \cos\phi} \right] \right] - \frac{1}{2} \delta(\mathbf{r} - \mathbf{r}'), \quad (2.4)$$

and K_1 is the modified Bessel function of first order. The δ function refers to a contour integral, not to a two-dimensional integral. Global mass conservation implies a sum rule for $h(\mathbf{r}, \mathbf{r}'; \mathbf{n}')$ which has been discussed in some detail in Ref. [20].

Equation (2.2) is an integro-differential equation for the interface position $\zeta(x)$, since both u and $\partial u / \partial n$ can be expressed via $\zeta(x)$ and its derivatives in a stationary situation. This is accomplished with the help of the Gibbs-Thomson and Stefan conditions, which read

$$u|_{\text{interface}} = \begin{cases} -\zeta/l_T^\alpha - d_0^\alpha \kappa, & \alpha \text{ phase} \\ \zeta/l_T^\beta + d_0^\beta \kappa, & \beta \text{ phase} \end{cases}, \quad (2.5)$$

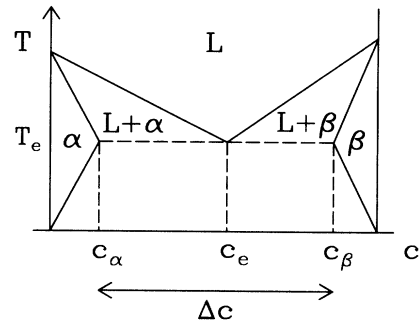


FIG. 1. Phase diagram of binary eutectic system. T is the temperature, c the concentration of one component. The regions L , α , and β correspond to one-phase equilibrium states of the liquid, the solid α , and the solid β phases, respectively. $L + \alpha$ and $L + \beta$ are regions of two-phase equilibrium between the liquid and one solid phase; the true concentrations of the two phases are given by the liquidus and solidus lines (solid lines) delimiting these regions. c_e , c_α , and c_β denote the equilibrium concentrations of the liquid and the two solid phases at the triple or eutectic point, whose temperature is T_e . Δc is the miscibility gap: $\Delta c = c_\beta - c_\alpha$.

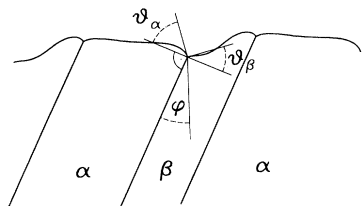


FIG. 2. Definition of the contact angles ϑ_α and ϑ_β , and the tilt angle ϕ . Note that ϕ is counted positive for a tilt to the right, while ϑ_α and ϑ_β are always positive.

$$-D \frac{\partial u}{\partial n} \Big|_{\text{interface}} = \begin{cases} [(1-k_\alpha)u + \delta]v_n, & \alpha \text{ phase} \\ [(1-k_\beta)u + \delta - 1]v_n, & \beta \text{ phase} \end{cases} \quad (2.6)$$

Here d_0^α and d_0^β are the capillary lengths for the two solid phases [19], κ is the interface curvature, l_T^α and l_T^β are the thermal lengths, D is the diffusion coefficient in the liquid, k_α and k_β are the partition coefficients, and $\delta = (c_e - c_\alpha)/\Delta c$ is the reduced miscibility gap for the α phase. The steady-state normal velocity v_n in the continuity equation (2.6) has a simple dependence on the interface shape

$$v_n = V(1 - \tan\phi \zeta_x)(1 + \zeta_x^2)^{-1/2}. \quad (2.7)$$

A final boundary condition is given by the requirement of mechanical equilibrium at the triple points, which determines the *contact angles* ϑ_α and ϑ_β at the triple points (see Fig. 2):

$$\begin{aligned} \gamma_{\alpha l} \sin(\vartheta_\alpha \mp \phi) + \gamma_{\beta l} \sin(\vartheta_\beta \pm \phi) &= \gamma_{\alpha\beta} \cos\phi, \\ \gamma_{\alpha l} \cos(\vartheta_\alpha \mp \phi) - \gamma_{\beta l} \cos(\vartheta_\beta \pm \phi) &= \pm \gamma_{\alpha\beta} \sin\phi. \end{aligned} \quad (2.8)$$

B. Numerical results

The numerical method to solve the integral equation (2.2) has been described in Ref. [19] for the symmetric case. There are some subtleties in finding asymmetric solutions, but we refrain from entering into these details (which have not been given elsewhere) to keep this paper concise.

To put our results in context, let us recall the structure of solution space for stationary lamellar growth [19,20]. It is summarized in Fig. 3, which shows the average undercooling as a function of the lamellar spacing at a fixed velocity. At small λ , we have four branches of *axisymmetric* solutions, which pairwise merge into fold singularities at roughly twice the wavelength corresponding to the minimum undercooling of the lowest branch. That is, we have a *discrete set* of solutions for each wavelength. It seems likely in the light of our knowledge about dendritic growth, where also a discrete solution set exists (which is infinite), that these four branches constitute only the beginning of an infinite ladder of solutions. Within numerical accuracy, it is hard to decide whether the fold singularities of the two pairs appear at exactly the same wavelength or not. Beyond the folds, no solutions with symmetric lamellae exist.

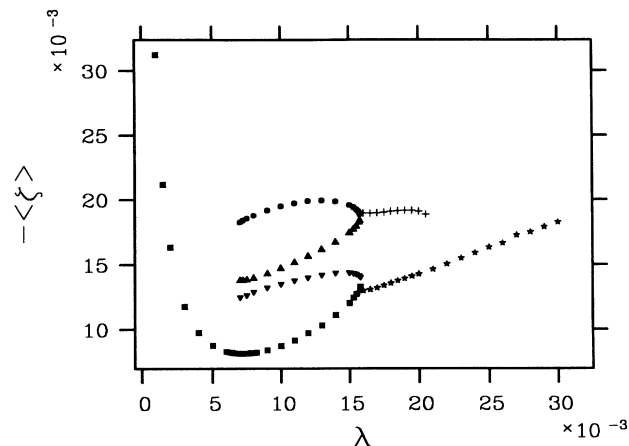


FIG. 3. Average undercooling as a function of λ for four branches of axisymmetric solutions to the model equations (squares, inverted triangles and triangles, and circles) and two branches of tilted solutions (stars, crosses). The symmetric branches form two pairs, whose members coalesce into fold singularities at $\lambda \approx 0.0158$. Beyond this λ value, no axisymmetric solutions could be found. $V=10.0$, material parameters: $d_0^\alpha = d_0^\beta = 10^{-5}$, $k_\alpha = 1.04$, $k_\beta = 1.04$, $u_\infty = 0.05$, $\delta = 0.3$, $\vartheta_\alpha = 0.9$, and $\vartheta_\beta = 0.7$. A similar structure, but with a subcritical upper tilted branch, was found for $V=27.5$, $d_0^\alpha = 2 \times 10^{-5}$, and $d_0^\beta = 5 \times 10^{-6}$.

The branch (characterized by stars in the figure) that bifurcates from the lowest symmetric branch and extends to wavelengths beyond the fold is also known from our previous work [19,20]. It consists of *tilted* solutions with globally broken parity. An example of a pattern from this branch is shown in Fig. 4. Note that the branch is twofold degenerate, since solutions tilted to the left and to the right have exactly the same undercooling, in a system with isotropic surface tension. We have verified that anisotropy removes this degeneracy [13], making it manifest that this branch actually consists of two.

Finally, the upper branch extending beyond the fold (denoted by crosses) is new. The characterization and discussion of solutions leading to this particular branch is the main purpose of this paper. Figure 5 shows a pattern from this branch, at the same wavelength that was considered in Fig. 4. Note that the lamellae of the α and β phases look as if they belonged to structures with opposite tilt orientations. This will become much more conspicuous in the case of a symmetric phase diagram considered below. Again, the branch is twofold degenerate, comprising solutions which can be obtained from each other by reflection with respect to the original symmetry axes.

The most appropriate (or fundamental) order parameter for these structures would be an amplitude of their antisymmetric part with respect to an axis in the middle of a lamella [30]. It might be calculated by integrating the square of the antisymmetric part over a period of the system. More easily calculated—and visualized—is the

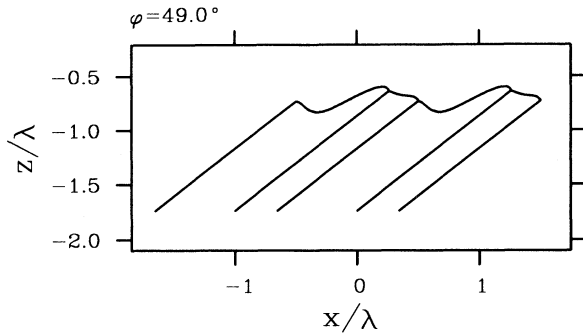


FIG. 4. Tilted pattern from the lower branch of Fig. 3. $\lambda=0.02$, $\phi=49.0^\circ$.

tilt angle, which in many cases may serve as an order parameter, too. The anomalous state (which appears in the case of symmetric eutectic systems) does not exhibit a tilt. Therefore, one has to describe its bifurcation by another quantity. One simple way is to use the height difference between the two triple points to the left and the right of, say, an α lamella. Both the tilt angle and the height difference are zero when each lamella is symmetric with respect to its center (the usual symmetric growth mode).

Figure 6 shows the tilt angle for the two broken-parity branches of Fig. 3. A few things should be noticed. First, the bifurcation appears at almost the same point and is supercritical for both branches. Second, the tilt angle of the upper branch is smaller than that of the lower one. Third, it does not increase monotonously as a function of λ in the whole range of λ values considered but decreases again at large λ .

As to the first point, our numerical accuracy does not permit a statement whether this is a case of “exact pseudobifurcality” (as explained before, we use the term pseudobifurcality to distinguish from true bifurcality, where both solutions have the same basic symmetric pattern). From our results for a symmetric phase diagram to be discussed below, this does not seem very likely, because there the difference between the two critical points is too large to be solely due to insufficient numerical accuracy (it is a five-percent effect, and our numerical resolution is on the order of one percent or better). On the oth-

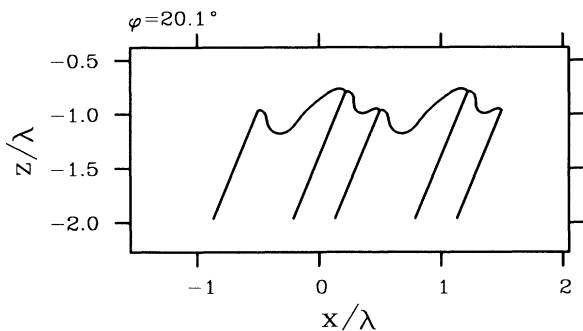


FIG. 5. Anomalous parity-breaking pattern from the upper branch of Fig. 3. $\lambda=0.02$, $\phi=20.1^\circ$.

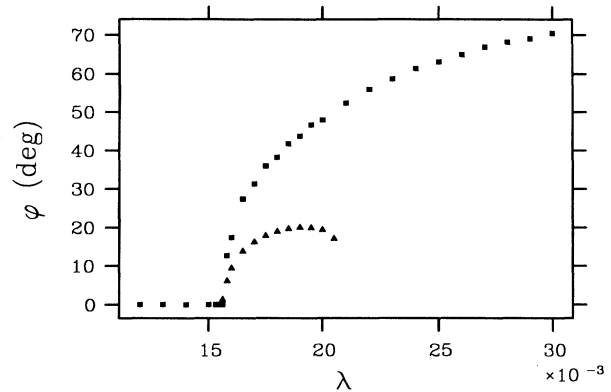


FIG. 6. Tilt angle as a function of lamella spacing for the two broken-parity branches of Fig. 3.

er hand, another case of an asymmetric phase diagram, with parameters very different from those of Fig. 3 (see the figure caption), again shows pseudobifurcality to within one to two percent of the wavelength, so that the symmetric case may be special in this respect. We conjecture that the bifurcation may be considered pseudobifurcality for all practical purposes if the phase diagram is nonsymmetric. As to the type of bifurcation, by which the *upper* tilted branch appears, this normally seems to be supercritical. We have seen a case of a slightly subcritical bifurcation for rather asymmetric system parameters (including different capillary lengths of the two phases).

The second of the aforementioned points will be discussed below. Regarding the third, shortly after the tilt angle starts to decrease, i.e., for λ values above $\lambda=0.0205$ [37], we do not find solutions anymore. Since it seems rather unlikely that the branch just ends there (without turning backward), it is tempting to conjecture that the persistent failure of convergence of the Newton solver (which is independent of the discretization mesh) is a signature of a new bifurcation. Such an interpretation is supported by past experience with the behavior of the iterative solver in the vicinity of bifurcations. However, without a good guess at the interface shape of the bifurcating solution it is hard to verify this conjecture.

Let us now turn to the symmetric phase diagram. Its bifurcation structure, evaluated for $c_\infty=c_e$ and given in Fig. 7, has not been discussed before. As was stated in Ref. [19], the competition between the effective interface stiffnesses of the α and β phases must lead to a qualitative change in the bifurcation diagram when the two phases become equivalent. Two out of the four *axisymmetric* branches become degenerate, so there appear to be only three branches. Plotted are, however, four—one of them as triangles with tip up, another with tip down. Their overlapping produces nice sixfold stars, even though the symmetry between the two phases has not explicitly been exploited in the numerical solution.

It is also this symmetry that is responsible for the fact that the solutions corresponding to the upper branch that extends beyond the fold singularity *are not tilted*. Figure 8 gives a pattern from the lower branch of ordinary tilted solutions, Fig. 9 one from the mentioned upper branch, at

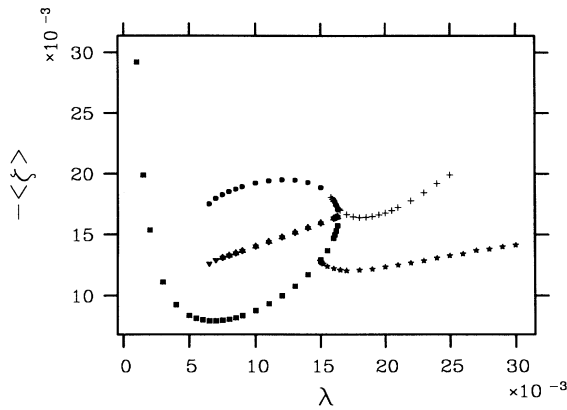


FIG. 7. The same as Fig. 3, but for a symmetric phase diagram and otherwise symmetric parameters: $d_0^\alpha = d_0^\beta = 10^{-5}$, $k_\alpha = k_\beta = 1$, $\vartheta_\alpha = \vartheta_\beta = 0.8$, $l_T^\alpha = l_T^\beta = 1$, $V = 10.0$, $u_\infty = 0$, and $\delta = 0.5$.

the same wavelength. In this symmetric case, for which an analytic treatment will be given below, the bifurcation to the upper branch is of standard supercritical type.

It is noteworthy that the parity-breaking bifurcation is still present in the fully symmetric system (see Fig. 8). This contrasts with Karma’s [15] random-walker model, according to which the tilting instability appears only for off-eutectic composition. Of course, we cannot exclude the possibility that in the symmetric system the tilted pattern becomes unstable against hard mode instabilities, and that therefore it could not be captured in Karma’s simulation. In order to make a definite statement one needs to perform a full linear stability analysis in all cases. There are, however, some remarks which should be made. First, in our analysis we have not seen that being at the eutectic concentration gives rise to any special event. Second, both numerically and analytically the symmetric system is found to support broken-parity solutions in a very similar manner as the nonsymmetric system. Third, tilted patterns manifest themselves in experimental situations as a robust feature. It is hard to imagine physically why this feature should disappear for the symmetric system. Moreover, as this paper was being written we received results of Monte Carlo simulations by

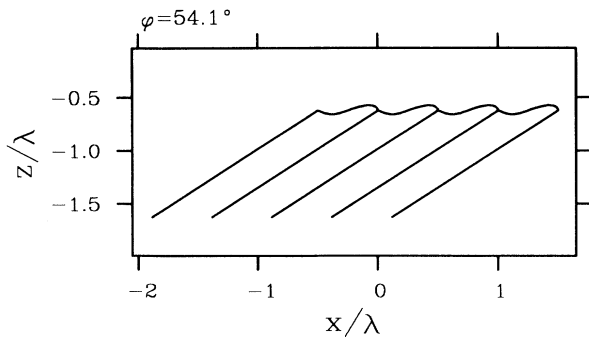


FIG. 8. Parity-breaking pattern from the lower branch of Fig. 7. The phase diagram is symmetric and the composition is that of the eutectic point ($u_\infty = 0$). $\lambda = 0.02$, $\phi = 54.1^\circ$.

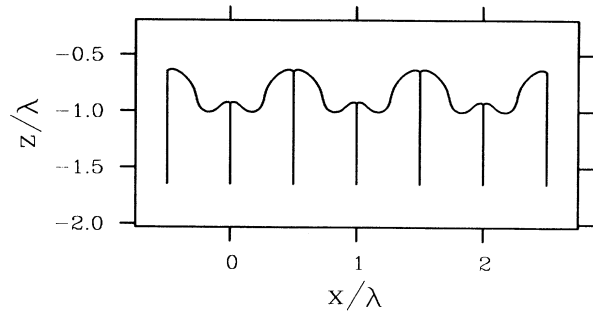


FIG. 9. Anomalous parity-breaking pattern from the upper branch of Fig. 7. $\lambda = 0.02$, $\phi = 0$.

Xiao, Alexander, and Rosenberger [38], who found that the tilting instability exists for completely symmetric systems, thus confirming our results.

Let us pursue the discussion of our results in the symmetric system. While the pattern of Fig. 9 cannot be characterized by a nonzero tilt angle, it definitely has lost axisymmetry with respect to the central axis of each single lamella [39]. That is, we have *local parity breaking*. Note that we can describe each of the branches by one of the simple order parameters introduced above, but that the other is zero. Furthermore, it is difficult to speak of the same critical point, since the bifurcation points of the two branches are roughly six percent of the wavelength apart.

It is amusing to note that solutions corresponding to this upper branch can be found in a JH-type theory of the simplest kind. By “simplest kind” we mean that, according to the original idea by JH, the diffusion field is replaced with that of a planar interface. Inserting this diffusion field in the left-hand side of Eq. (2.5), one has, instead of an integral equation, two second-order ordinary differential equations

$$d_0^i \frac{\xi_{xx}}{(1 + \xi_x^2)^{3/2}} - \frac{\xi}{l_T^i} = \epsilon_i u(x, \xi(x)), \quad i = \alpha, \beta, \quad (2.9)$$

where $\epsilon_\alpha = 1$ and $\epsilon_\beta = -1$. The simplification arises be-

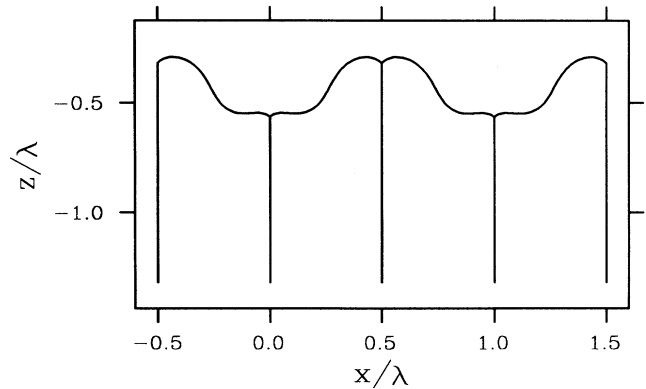


FIG. 10. Anomalous parity-breaking pattern from a Jackson-Hunt-type theory with planar front diffusion field. $\lambda = 0.02$, $\phi = 0$.

cause the (now) right-hand side is a known function. Ordinarily, one even replaces the function $\zeta(x)$ on the right-hand side by the position $\bar{\zeta}$ of the planar interface, which means dropping the z dependence of the diffusion field (this was also the approximation used in Ref. [19]). Let us call this the first type of a JH theory of the simplest kind. The second type then consists in carrying along the $\zeta(x)$ on the right-hand side, and it is this type that has solutions exhibiting local parity breaking. An example is given in Fig. 10. In Sec. IV we will develop an analytic theory to account for the transition to the anomalous state, within a more refined theory of the JH type (which is no longer of the simplest kind).

III. PHENOMENOLOGY OF PSEUDO-BICRITICALITY AND EXPERIMENTAL ACCESS TO THE NEW BRANCH

In this section we would like to present a phenomenological discussion of the (pseudo)bicritical feature of the broken-parity state. We will also suggest an experimental procedure to realize the new state.

We have seen in the last section that at the critical point two broken-parity solutions merge in a (normally) supercritical manner. If one concentrates on one branch only (say the old one), the normal form of the Landau expansion compatible with symmetries reads to leading order for the orderlike parameter ϕ

$$\tau_1 \dot{\phi} = \mu\phi - \alpha_1 \phi^3, \quad (3.1)$$

where μ stands for the bifurcation parameter (it vanishes at the bifurcation point), α is the Landau constant, assumed to be positive to account for a supercritical bifurcation, and τ is some time scale for the motion of interest. As we are interested in homogeneous parity-breaking bifurcations, there is no need to include a term describing wall effects. The second solution merging at the same point is described by a similar normal form

$$\tau_2 \dot{\phi} = \mu\phi - \alpha_2 \phi^3. \quad (3.2)$$

Since the new branch has a smaller tilt angle (see Fig. 6), we have $\alpha_2 > \alpha_1$.

An interesting feature of the Landau expansion for a stationary bifurcation is that it can be cast into a variational formulation

$$\tau_i \dot{\phi} = - \frac{\partial}{\partial \phi} F_i, \quad (3.3)$$

where

$$F_i(\phi) = -\frac{1}{2}\mu\phi^2 + \frac{1}{4}\alpha_i\phi^4, \quad i = 1, 2. \quad (3.4)$$

The quantity F can be thought of as the kinetic analogue of a thermodynamical potential. More precisely, the evolution equation for F_i is

$$\frac{\partial F_i}{\partial t} = \frac{\partial F_i}{\partial \phi} \frac{\partial \phi}{\partial t} = - \frac{1}{\tau_i} \left[\frac{\partial F_i}{\partial \phi} \right]^2 \leq 0, \quad (3.5)$$

where use has been made of Eq. (3.3). This result means that the function F is a nonincreasing function of time.

This is the Lyapunov function. As a consequence, we expect the system to evolve towards the state that minimizes the Lyapunov function. The two stationary solutions of Eqs. (3.1) and (3.2) are given by

$$\phi_1 = (\mu/\alpha_1)^{1/2}, \quad \phi_2 = (\mu/\alpha_2)^{1/2}, \quad (3.6)$$

not counting the negative solutions. The Lyapunov function has the following values for these solutions:

$$F_1 = -\frac{\mu^2}{2\alpha_1}, \quad F_2 = -\frac{\mu^2}{2\alpha_2}. \quad (3.7)$$

Since $\alpha_2 > \alpha_1$, one has $F_2 > F_1$; i.e., the second branch has a higher “energy,” or, in other words, is metastable. This simple phenomenology shows us that the old branch is more favorable than the new one. It is worth mentioning, however, that comparing the “free energies” is somehow misleading in the frame of deterministic dynamics. Indeed, the final state should depend on initial conditions only and not on comparing various “energies.” Of course, fluctuations, which are not accounted for, may change such a conclusion. There are, however, some indications on the way by which to prepare a system, confirmed by experimental observations, to have access to such or such a state. Some of these questions will be discussed below.

As shown in Fig. 3 the new tilted branch (crosses) has a higher undercooling than the old one (stars). There exists agreement in the metallurgical literature that out of two possible states a system chooses the one which corresponds to the smaller undercooling. This criterion is also in favor of the old branch, since it has a lower undercooling.

Of course, the absolute minimum in Fig. 3 corresponds to a symmetric state and one would expect—with the proviso one admits the minimum undercooling principle—that state to prevail always. This is not yet clear, however. Indeed, according to one of our previous analyses [20] we have proposed how to destabilize the whole symmetric front against parity breaking, a suggestion which has found an impressive experimental confirmation [27]. This consisted simply in a sudden increase of the pulling speed by a factor of about 4. Indeed, since the quantity $\lambda^2 V$ is approximately a constant of motion, a sudden jump of V by a factor of 4 would imply a reduction of the wavelength by a factor of 2, in a situation where the response of the periodic structure is instantaneous. This is not the case. Indeed, the wavelength adjustment is a very slow process (at least of the order of many minutes or even an hour) so that the front would temporarily “feel” that for the actual velocity the wavelength is twice too large. Our analysis tells us that in such a situation the front should undergo a parity-breaking bifurcation. This is what the experiment has indeed shown.

In the absence of a full linear stability analysis of the tilted pattern we cannot exclude the possibility that the asymmetric pattern is a transient and after some time the system would go back to the symmetric state. For such a process to be operative the wavelength should be approximately halved. Such a wavelength reduction occurs ba-

sically via phase diffusion, expressing the Eckhaus instability. This mechanism seems extremely slow so that for a given experiment, once the tilted pattern takes place, there is no chance to observe a transition back to the symmetric state, except after a strong variation of the growth velocity (by suddenly reducing it by a factor of approximately 4).

Now in the light of the results reported in the present paper we can legitimately ask the following question: why does the system choose the lower tilted branch and not the upper one after a sudden velocity increase? The answer is quite clear. Figure 11 schematically shows the situation. V_1 designates the original velocity, while $V_2 = 4V_1$. S_1 denotes the representative point of the symmetric state at V_1 (this point is close to the minimum undercooling point). If the velocity change were slow enough, going adiabatically from V_1 to $V_2 = 4V_1$, then the final state would have S_2 as a representative point; that is to say, the state would be a symmetric pattern at the minimum undercooling corresponding to $V = V_2$. If, on the contrary, the velocity jump is sudden, going from V_1 to V_2 , then temporarily the wavelength will still be $\lambda_{1\min}$. For the solid to grow in a stationary manner at this couple $(V_2, \lambda_{1\min})$, the undercooling should adapt itself such that now the representing point is S'_1 . Our theory tells us that point S'_1 is close to the instability against parity-breaking fluctuations. Then the symmetric pattern loses its stability and a tilted pattern develops. It should be added that since parity breaking is a normal bifurcation, the growth of the asymmetric perturbation is exponentially fast, while wavelength adjustment is of the diffusive type and is very slow compared to the birth of the broken-parity state. Thus by this process one is naturally led to the lower branch of broken-parity states. This is what the experiment of Faivre and Mergy [27] has confirmed.

How to get to the upper branch? A simple experimental protocol would be the following. Once the front has reached the lower broken-parity branch at S'_1 (as described above), one should, keeping the same pulling speed, undercool the front in a controlled way to reach

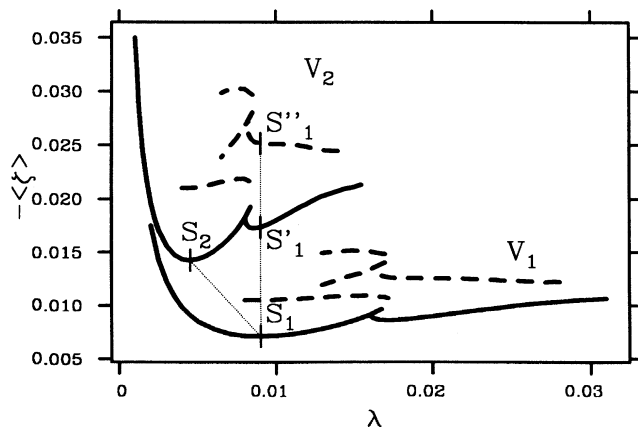


FIG. 11. Schematic plot describing the representative points of different states that are reached by the system depending on the experimental protocol (see text).

the point S''_1 in Fig. 11. Figure 3 shows that close to the critical point for the birth of tilted states the upper branch has an undercooling which is approximately 1.5 times that of the lower branch: the average front position for the lower branch is about 0.013 in the chosen units (see [37] $[-\langle\xi\rangle = \langle\Delta T\rangle/G]$), while that of the upper branch is about 0.019. Thus, knowing approximately the absolute temperature of the front in the lower branch and the eutectic temperature, we obtain the undercooling in degrees as their difference and can then determine the temperature of the upper branch via an increase of the temperature difference by a factor of 1.5.

The method by which the front can temporarily be undercooled down to the upper-branch temperature may be the following. Heating locally along, and close enough to, the front, for example by a laser source, would cause melting resulting into a recession of the front towards the cold contact. If the laser pulse is localized enough so that the heat produced can equilibrate very fast with the environment, it should put the system temporarily in a higher undercooling. Indeed, the front which had receded towards the cold contact (due to melting) may still be in a transient state with a temperature below the melting temperature imposed by the hot and cold contacts. If the increase of the undercooling is large enough we expect the new state to manifest itself. Another interesting possibility to undercool the front should be provided by the experimental setup of Oswald [40]. The sample there is, besides the usual thermal contacts, supported by a thin metallic plate (actually a metallic deposit) where electric currents are used to heat the sample. The metallic plate reaches thermal equilibrium with the environment faster than the sample itself, so that the front can, temporarily, be significantly undercooled after sudden removal of the electric power.

We believe that the above suggested protocols should constitute important tools towards the understanding of the variety of the fascinating patterns in eutectic growth. Besides the access to the upper branch of the tilted state, the same protocol can be used to investigate the existence of higher branches of symmetric patterns that are exhibited on Fig. 3. In this situation one should start from a symmetric pattern and suddenly undercool the front. By looking to Fig. 3, it is a simple matter to estimate the front temperature associated with each branch.

IV. ANALYTIC TREATMENT FOR TRANSITION TO THE ANOMALOUS STATE

We have seen from our full numerical results that in the particular case where both solid phases are identical, the upper broken-parity state branch corresponds to untilted asymmetric solutions, the so-called anomalous states. We would like to develop here an analytic treatment accounting for the transition to the anomalous state. We will adopt the same spirit as the one used for the parity-breaking transition in Ref. [22]. There we have considered the simplest next step of analysis beyond that of JH. In order to determine the diffusion field, we have included an antisymmetric component in the front profile. This treatment has proven to be fruitful since we

recovered the essential features of parity breaking found numerically. This gives a strong hint that a similar treatment, which would consist in including a local asymmetry in the front profile, should capture the main features of the transition to the anomalous state.

We consider here the same standard simplifications as those used in Sec. II. But, since our aim is to deal with the transition to the anomalous state, we will, because of the very nature of the state we want to investigate, look at symmetric eutectic systems. Furthermore, we shall assume that the system grows in an isothermal environment. This assumption is legitimate, since in standard directional eutectic growth experiments the thermal length is much larger than the wavelength of the pattern. We will also assume that the concentration gap for each phase (i.e., $c_s^\alpha - c_l$ and $c_s^\beta - c_l$) is constant. This means in our notation that the partition coefficients k_α and k_β will be both taken equal to 1.

For clarity, we rewrite the growth equations in the present context. Since we are interested in the transition to the anomalous state, the tilt angle is zero. The diffusion equation then becomes (taking the diffusion length as length unit)

$$\nabla^2 u + 2u_z = 0. \quad (4.1)$$

Using the fact that both solid phases are identical (i.e., $d_0^\alpha = d_0^\beta = d_0$ and $\delta = \frac{1}{2}$) and that $k_\alpha = k_\beta = 1$, the Gibbs-Thomson and conservation conditions at the interface $z = \zeta(x)$ take the following form (with $D = 1$):

$$u = \pm(\Delta - d_0\kappa), \quad (4.2)$$

$$u_z - \zeta_x u_x = \mp 1. \quad (4.3)$$

The upper and lower signs refer to the solid phase with the lower and the higher concentrations, respectively.

In the situation where the solid grows in an isothermal environment, Δ designates the dimensionless undercooling [$\Delta = (T_e - T_0)/m\Delta c$, where T_0 is the temperature in which the solid evolves]. In directional growth, Δ should be replaced by $-\zeta/l_T$. However, for all practical purposes we can write $\zeta/l_T \simeq \bar{\zeta}/l_T$, which simply means that the front can be viewed to be, practically, in an isothermal environment. This is justified by the fact that the front excursion, which is of the order of λ , is much smaller than the thermal length ($l_T \sim 1$ while $\lambda \sim 10^{-2}$; recall that both quantities are measured in the unit of the diffusion length). To sum up, in the case of directional growth Δ can be thought of as a measure of the average position. To complete our set of equations we should write down the mechanical equilibrium conditions at the triple points where the three phases intersect:

$$\zeta_x(0) = \tan(\theta), \quad \zeta_x(\lambda/2) = -\tan(\theta), \quad (4.4)$$

where θ is the contact angle at the triple point.

To determine the diffusion field for axisymmetric states, Jackson and Hunt assume a planar front. That is, they solve Eq. (4.1) subject to condition (4.3) at $\zeta = \bar{\zeta}$, $u_z(\bar{\zeta}) = \mp 1$. Here we use a strategy analogous to that employed in [22] in the context of parity breaking. It consists in replacing the actual diffusion field by that of a

lamellar structure, whose front is made of straight segments (to be defined below). The main characteristic of the anomalous states is that two consecutive triple points of the front are not at the same height. So the ansatz consists of assuming that the interface over one period consists of four straight segments defined by

$$\zeta(z) - \bar{\zeta} = \begin{cases} -\frac{y_0}{2} + x \tan\theta, & 0 \leq x \leq x_0 \\ \frac{y_0}{2} + (\lambda/2 - x) \tan\theta, & x_0 \leq x \leq \lambda/2 \end{cases} \quad (4.5)$$

$$\zeta(z) - \bar{\zeta} = \begin{cases} \frac{y_0}{2} + (\lambda/2 - x) \tan\theta, & x_0 \leq x \leq \lambda/2 \\ -\frac{y_0}{2} + (\lambda - x) \tan\theta, & \lambda - x_0 \leq x \leq \lambda \end{cases} \quad (4.6)$$

for the α -liquid interface and by

$$\zeta(x) - \bar{\zeta} = \begin{cases} \frac{y_0}{2} + (x - \lambda/2) \tan\theta, & \lambda/2 \leq x \leq \lambda - x_0 \\ -\frac{y_0}{2} + (\lambda - x) \tan\theta, & \lambda - x_0 \leq x \leq \lambda \end{cases} \quad (4.7)$$

$$\zeta(x) - \bar{\zeta} = \begin{cases} \frac{y_0}{2} + (x - \lambda/2) \tan\theta, & \lambda/2 \leq x \leq \lambda - x_0 \\ -\frac{y_0}{2} + (\lambda - x) \tan\theta, & \lambda - x_0 \leq x \leq \lambda \end{cases} \quad (4.8)$$

for the β -liquid interface. The quantity y_0 is the height difference between two consecutive triple points (see Fig. 12), and x_0 and $\lambda - x_0$ are the positions of the two intersection points [$x_0 = \lambda/4 + y_0/(2 \tan\theta)$]. Note that the triple points sit at a height of $\pm y_0/2$ (measured from the reference position $\bar{\zeta}$). This choice is made in order to keep the symmetry between a solution with height difference y_0 and one with $-y_0$ [see the remark below after Eq. (4.25)]. This profile has the property that each lamella is asymmetric with respect to its center and is a mirror image of the other lamella. Note also that this front profile satisfies the mechanical equilibrium condition [Eq. (4.4)].

The main part of the work is to determine the diffusion field corresponding to the front defined above. We can write the general solution of the stationary diffusion equation [Eq. (4.1)] for a spatially periodic system as

$$u(x, z) = \sum_n C_n e^{ik_n x} e^{-Q_n(z - \bar{\zeta})}, \quad (4.9)$$

where $k_n = 2\pi n/\lambda$, $Q_n = 1 + \sqrt{1 + k_n^2}$, and C_n are undetermined coefficients for the moment. In the (standard)

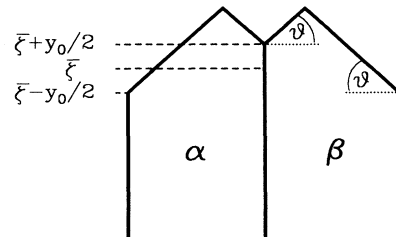


FIG. 12. Scheme of the front used to determine the diffusion field.

small-Péclet-number limit $Q_n \simeq |k_n|$ for $n \neq 0$ ($Q_0 = 2$). Both in Refs. [11] and [19], $\underline{\xi}$ has been considered the average interface position. However, taking $\underline{\xi}$ larger than the *minimum* interface position ξ_{\min} and evaluating the C_n for $\xi = \underline{\xi}$ would lead to a Fourier series, which diverges for $\xi < \underline{\xi}$, spoiling the general validity of the ansatz. For a *planar* front, ξ_{\min} is identical to the *average* interface position $\langle \xi \rangle$ and the *reference* position $\bar{\xi}$ defined above. Since we will expand about the Jackson-Hunt solution in the following, we can identify $\underline{\xi}$ and $\bar{\xi}$.

The coefficients C_n are obtained from the continuity equation (4.3). But in its actual form, it is difficult to exploit because all the quantities involved in this equation have to be evaluated along the front. Our procedure is to determine the diffusion field to leading order in the deviation from a JH theory. This is to say that we expand the continuity equation in the front deviation $\xi - \bar{\xi}$ and, since this quantity is of the order of Péclet number, the remaining terms would produce higher-order contributions in the Péclet number.

To leading order, the continuity equation takes, in an α

lamella, for example, the form

$$u_z = -(\xi - \bar{\xi})u_{zz}^{(0)} + \xi_x u_x^{(0)} - 1, \quad (4.10)$$

where the fields on both sides are understood to be evaluated at $z = \bar{\xi}$. The quantity $u^{(0)}$ refers to the JH field and its expression is given by

$$u^{(0)}(x, z) = \sum_{n \neq 0} B_n e^{ik_n x} e^{-Q_n(z - \bar{\xi})}, \quad (4.11)$$

where

$$B_n = \frac{4e^{-in\pi/2}}{\lambda k_n Q_n} \sin(n\pi/2). \quad (4.12)$$

One can now obtain the coefficients C_n by inserting (4.9) into the continuity equation (4.10). After lengthy algebra, this procedure yields

$$C_n = C_n^{(1)} + C_n^{(2)} + C_n^{(3)}, \quad (4.13)$$

with

$$C_n^{(1)} = -\frac{2i}{\lambda Q_n k_n} [1 - (-1)^n], \quad (4.14)$$

$$C_n^{(2)} = -\frac{2B_n}{\lambda Q_n} \tan(\theta) [1 - \cos(2k_n x_0)] - \frac{1}{\lambda Q_n} \sum_{m > 0, m \neq n} 4k_m B_m \tan(\theta) \left[\frac{1}{k_m - k_n} \left[\cos[(k_m - k_n)x_0] - \frac{1 + (-1)^{m-n}}{2} \right] - \frac{1}{k_m + k_n} \left[\cos[(k_m + k_n)x_0] - \frac{1 + (-1)^{m-n}}{2} \right] \right], \quad (4.15)$$

$$C_n^{(3)} = -\frac{Q_n B_n}{\lambda} \tan(\theta) \left[x_0^2 + \left[\frac{\lambda}{2} - x_0 \right]^2 + \frac{1}{k_n^2} [1 - \cos(2k_n x_0)] \right] - \frac{1}{\lambda Q_n} \sum_{m > 0, m \neq n} 4Q_m^2 B_m \tan(\theta) \left[\frac{1}{(k_m - k_n)^2} \left[\cos[(k_m - k_n)x_0] - \frac{1 + (-1)^{m-n}}{2} \right] - \frac{1}{(k_m + k_n)^2} \left[\cos[(k_m + k_n)x_0] - \frac{1 + (-1)^{m-n}}{2} \right] \right]. \quad (4.16)$$

Making use of the expression of the coefficients B_n , we can rewrite the diffusion field at $z = \bar{\xi}$ in a much more compact form:

$$u(x) = \sum_{n > 0} D_n \sin \left[\frac{2\pi n x}{\lambda} \right], \quad (4.17)$$

with

$$D_{2n-1} = \frac{2\lambda}{\pi^2 (2n-1)^2} - 4\lambda \tan(\theta) \sum_{m=1}^{\infty} \frac{1 - (-1)^m \cos(4\pi m y)}{\pi^3 m [4m^2 - (2n-1)^2]} + \frac{\lambda}{2\pi(2n-1)} \tan(\theta) + 2\lambda \tan(\theta) \sum_{m=1}^{n-1} \frac{1 - (-1)^m \cos(4\pi m y)}{\pi^3 m^2 [2m - (2n-1)]} + \frac{8\lambda y^2}{\pi(2n-1)} \tan(\theta), \quad (4.18)$$

$$D_{2n} = 8\lambda \tan(\theta) \sum_{m=1}^{\infty} \frac{(-1)^m \sin[2\pi(2m-1)y]}{\pi^3 (2m-1)(2m-2n-1)(2m+2n-1)}, \quad (4.19)$$

where $y = y_0 / (2\lambda \tan\theta)$. Note that D_{2n-1} and D_{2n} are even and odd analytic functions of y , respectively.

Our analytic treatment can be pursued much further. Before proceeding further, some remarks are in order. Having obtained the diffusion field, we can in principle solve for the front profile, which is compatible with that field. For that purpose we should insert the expression of the diffusion field [Eq. (4.17)] into the Gibbs-Thomson equation [Eq. (4.2)]. The determination of the front profile then amounts to solving a nonlinear differential equation subject to the mechanical boundary conditions [Eq. (4.4)]. Using the expression of the curvature, (4.2) reads

$$d_0 \frac{\xi_{xx}}{(1 + \xi_x^2)^{3/2}} + \Delta = \pm u(x, y_0), \quad (4.20)$$

where y_0 has been put explicitly in the argument of the diffusion field to remind us that u is parametrized by y_0 . The integration of this second-order equation over a half-period requires the determination of two integration constants, which are furnished by the two boundary conditions on the slope ξ_x at the triple point. At that stage y_0 would still be undetermined. So it seems as if the present problem could be solved for arbitrary values of y_0 , since we have made no assumption on y_0 . This is, fortunately, not the case. For the self-consistency of the problem, we have to impose, in addition to mechanical equilibrium, that the two ends on a given lamella [e.g., $\xi(0)$ and $\xi(\lambda/2)$] of the front profile which solves (4.2) subject to (4.4) must have a height difference equal to y_0 . This additional condition can be written simply as

$$\xi(\lambda/2, y_0) - \xi(0, y_0) = y_0, \quad (4.21)$$

where again we put y_0 explicitly in the argument, for the same reasons we mentioned above.

The above equation is sort of a nonlinear eigenvalue problem of the Barenblat-Zeldovich type. It leads generically to the selection of a discrete set of y_0 values. The quantity y_0 can be thought of as an order parameter for the anomalous state. Indeed, in the usual symmetric state $y_0 = 0$, while anomalous states are characterized by nonzero values of y_0 .

Let us now come back to the analytic analysis of the bifurcation. In order to determine the bifurcation point where the axisymmetric state undergoes a local parity-breaking transition (characterized by a nonzero value of y_0), we need to determine whether Eq. (4.21) is satisfied for a nontrivial value of y_0 . The procedure is as follows. Equation (4.2) can be integrated once over x (from 0 to x , where we make use of the mechanical equilibrium condition at $x = 0$). It gives

$$\frac{\xi_x}{\sqrt{1 + \xi_x^2}} = \sin(\theta) + \int_0^x \frac{u - \Delta}{d_0} dx \equiv f(x). \quad (4.22)$$

The slope ξ_x can be expressed as a function of f , and a second integration over a half-period can be achieved to obtain

$$\xi(\lambda/2, y_0) - \xi(0, y_0) = \int_0^{\lambda/2} \frac{f(x)}{\sqrt{1 - f^2}} dx \equiv F(y_0, \lambda, \mu), \quad (4.23)$$

where μ stands for the material and control parameters (e.g., d_0 , θ , and l). Finally, the self-consistency equation (4.21) can be written as follows:

$$F(y_0, \lambda, \mu) = y_0. \quad (4.24)$$

This equation is a general expression for the parameter y_0 as function of the other parameters. Before exploiting it, let us derive the equation that relates the undercooling to the other parameters. For that purpose we average Eq. (4.2) over one period (actually over a half-period, because the two solid phases are identical). The result is

$$\Delta = \frac{4d_0}{\lambda} \sin(\theta) + 2 \sum_{n=1}^{\infty} \frac{D_{2n-1}}{\pi(2n-1)}. \quad (4.25)$$

Equations (4.24) and (4.25) are general expressions which determine y_0 and Δ as a function of the other parameters.

One can easily check that $\Delta(-y_0) = \Delta(y_0)$, as it should be. One understands readily that the undercooling has to be an even function, because the anomalous states associated with opposite values of the order parameter are identical: they are deduced from each other by a translation of a half-period. One finds also that F , as it should be, has a well-defined parity, $F(-y_0) = -F(y_0)$, but the verification is not straightforward (see the Appendix). Using the parity of F , we can see that for an axisymmetric state (i.e., $y_0 = 0$) the self-consistency relation is always satisfied [$F(y_0 = 0) = 0$].

In order to investigate the possibility for the symmetric front to undergo a transition to the anomalous state, we have to find for which values of the parameters λ and μ the self-consistency relation is satisfied for a nontrivial value of the order parameter y_0 . This can be done numerically in the general case, but in order to go further in the analytic treatment, we will first confine ourselves to small contact angles, where the calculation of the critical point turns out to be simple. This restriction amounts to neglecting f^2 against 1 in the square root appearing in Eq. (4.23). The justification of this assumption is as follows. Indeed, if we evaluate the order of magnitude of the function f in the simple case of the symmetric growth (i.e., by using the JH diffusion field), we find that $f \sim \lambda^2 / (\pi^3 d_0)$. If our model correctly contains the principal ingredients we expect the critical wavelength λ_c to be of the order of the JH minimum undercooling wavelength λ_{\min} ($\lambda_c \sim 2\lambda_{\min}$), as in the full calculation. Using the expression of λ_{\min} ($\lambda_{\min}^2 \simeq \pi^3 d_0 \sin\theta$), we find that f is of order $\sin\theta$. So, for small θ , f should be reasonably small. In this limit the function F reads

$$F(y_0, \lambda, \mu) = \frac{\lambda^2}{8d_0} \sum_{n=1}^{\infty} \frac{D_{2n}}{\pi n}, \quad (4.26)$$

where use has been made of Eq. (4.25). We can write F in a more usable form:

$$F(y_0, \lambda, \mu) = \frac{2\lambda \tan(\theta)}{\sigma^2} G \left[\frac{y_0}{2\lambda \tan(\theta)} \right], \quad (4.27)$$

with

$G(y)$

$$= \frac{1}{2} \sum_{n=1}^{\infty} \sum_{m=1}^{\infty} \frac{(-1)^m \sin[2\pi(2m-1)y]}{\pi^4 n(2m-1)(2m-2n-1)(2m+2n-1)} \quad (4.28)$$

and $\sigma^2 \equiv d_0/\lambda^2$. The self-consistency relation then becomes

$$G(y) = \sigma^2 y, \quad (4.29)$$

with $y = y_0 / (2\lambda \tan\theta)$.

The resolution of this equation can be achieved graphically. It suffices to determine the intersection point between the curve $G(y)$ and the set of straight lines parametrized by their slope σ^2 . As shown in Fig. 13, for values of σ bigger than a certain critical value σ_c (to be defined below) there is only a single solution $y=0$, and for $\sigma < \sigma_c$, in addition to the trivial solution, a second solution $y \neq 0$ appears. When $\sigma = \sigma_c$, we are in the critical situation where the straight line is tangent to the curve G at the point $y=0$. As a summary, the bifurcation occurs below the critical value σ_c given by

$$\sigma_c = \frac{\alpha_1}{\pi^3}, \quad (4.30)$$

with

$$\alpha_1 \equiv \sum_{n=1}^{\infty} \sum_{m=1}^{\infty} \frac{(-1)^m}{n(2m-2n-1)(2m+2n-1)} \approx 0.45, \quad (4.31)$$

and it is supercritical, since y goes continuously from 0 to a nonzero value. The bifurcation diagram is shown in Fig. 14. The horizontal axis represents $\sigma^{-1/2}$, which varies linearly with λ . In reality, there is also a bifurcation branch in the region where y_0 is negative. The bifurcation curve is symmetric with respect to the horizontal axis, since G is an odd function of y_0 . For a given value of σ ($< \sigma_c \approx 0.01$), there are two anomalous states associ-

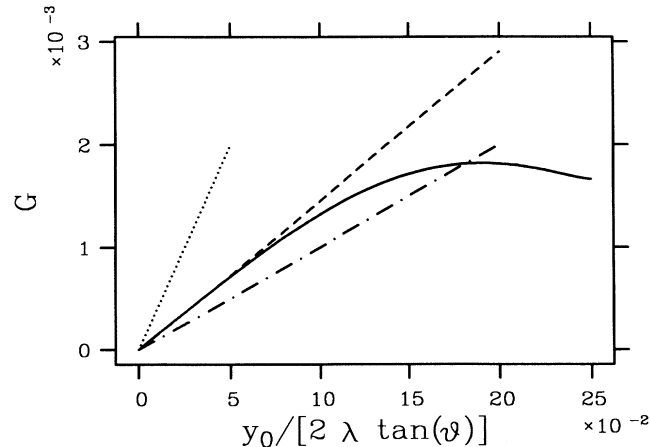


FIG. 13. Curve representing the function G vs y . In addition are plotted three straight lines with respective slopes $\sigma^2 > \sigma_c^2$ (dotted line), $\sigma^2 = \sigma_c^2$ (dashed line), and $\sigma^2 < \sigma_c^2$ (dotted-dashed line).

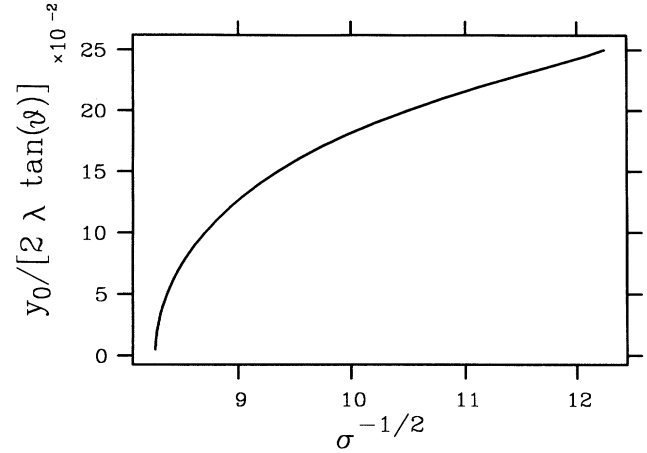


FIG. 14. Bifurcation curve showing the height difference between two consecutive triple points as a function of $\sigma^{-1/2}$.

ated with opposite values of the order parameter y_0 . Using the definition of σ we can restate the result as follows: for a given velocity, the initially symmetric solution loses its stability against “anomalous” fluctuations for $\lambda > \tilde{\lambda}_c = (2d_0 D / V \sigma_c)^{1/2}$. The tilted variables refer to the physical ones.

We can compare the critical wavelength λ_c with the JH minimum undercooling wavelength λ_{\min} (which corresponds to the JH symmetric front with the minimum undercooling). We find that $\lambda_c / \lambda_{\min} \sim 1.5 / \sqrt{\sin(\theta)}$. This result means that the parity symmetry is lost at a wavelength larger than λ_{\min} , that is, in a regime where the front dynamics are dominated by diffusion. This feature agrees with the full numerical analysis.

Let us now examine the general case where θ is not necessary small. We compute the exact expression of F [Eq. (4.24)] for given values of the contact angle and solve numerically the self-consistency equation, which is a simple nonlinear algebraic equation. For small θ ($\theta=0.01$), we recover exactly the same bifurcation diagram shown in Fig. 14. As θ increases (from $\theta=0.1$ to 0.8), the criti-

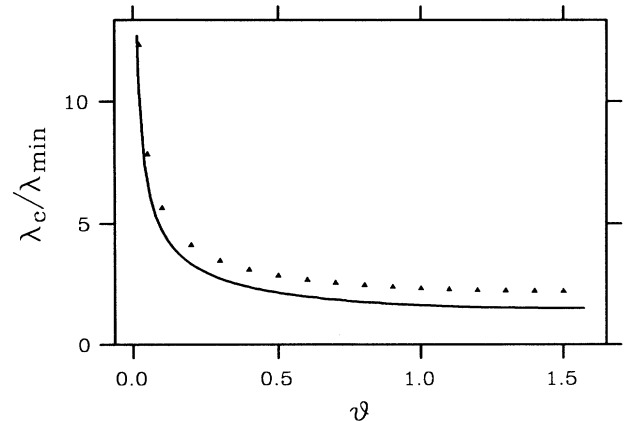


FIG. 15. Ratio of the critical wavelength for the appearance of the anomalous state to that corresponding to minimum undercooling in the JH theory vs the contact angle in both analytic (triangles) and full numerical (solid line) cases.

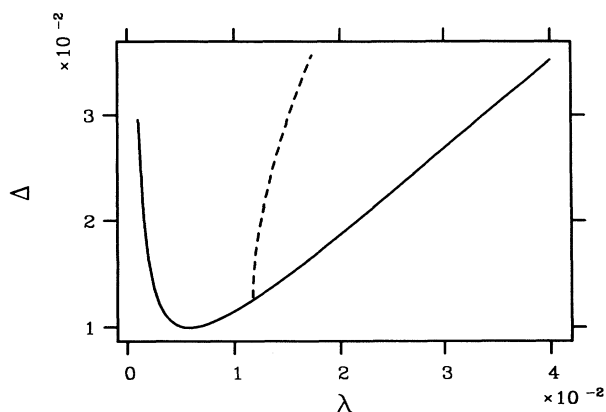


FIG. 16. Undercooling as a function of λ for axisymmetric states (solid line) and anomalous states (dashed line).

cal wavelength decreases slightly but the bifurcating curve does not qualitatively and even quantitatively change. We can therefore extrapolate the analytic expression of the ratio λ_c/λ_{\min} for a bigger contact angle θ without committing large errors. In Fig. 15 we have plotted this ratio as a function of θ and compare it with that found from the full numerical calculation. We can see that the agreement is very good and that for $\theta=0.8$ we find a ratio approximately equal to 2, as in the full calculation.

It is also interesting to know how the undercooling is modified above the transition to the anomalous state. Using the obtained bifurcation diagrams, which give y_0 versus λ , we can perform the calculation of expression (4.25). The result is given in Fig. 16, which shows both the undercooling of the symmetric and asymmetric fronts against the wavelength. We recognize the classical branch associated with symmetric states. In addition, we observe a branch emerging from the main one at the critical wavelength λ_c , determined above. This new branch corresponds to the existence of anomalous states. We can also note that the anomalous states are more undercooled than the symmetric ones for a fixed wavelength. Of course, this treatment does not account for the fact that the anomalous state does not merge from the lower sym-

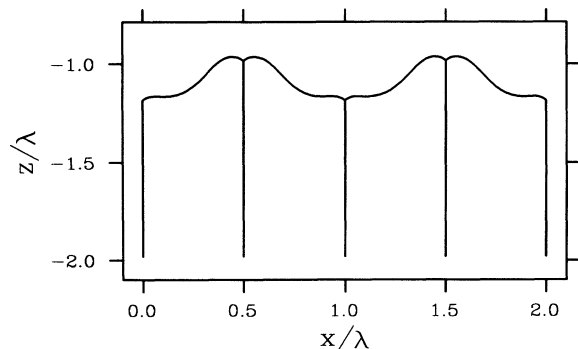


FIG. 17. A typical anomalous front profile computed for $d_0=10^{-5}$, $\vartheta=0.8$, $l_T=1$, and $y_0/\lambda=0.2$ in the context of the analytic theory.

metric state branch but from the upper one. However, the increase of the undercooling at the transition seems to be consistent with the full numerical calculations, which predict that the anomalous states appear from the upper symmetric state branch, sitting at higher undercooling.

As we have seen before, the determination of the profile amounts to solving a nonlinear differential equation [Eq. (4.2)] subject to a mechanical equilibrium condition [Eq. (4.4)] and to the self-consistency condition [Eq. (4.21)]. This problem can easily be solved numerically by means of a shooting method. Shown in Fig. 17 is a typical “anomalous” front profile. The morphology of this state is similar to that found from the full numerical calculation (Fig. 9).

V. CONCLUSION

We have shown from the integral formulation that the eutectic problem exhibits pseudobcritical features: two broken-parity states admix simultaneously at the same critical point as a forward bifurcation. The critical point is typically located, for a given velocity, at a wavelength which is approximately twice the one that provides the minimum undercooling for the symmetric pattern.

In the special situation where both solid phases have exactly the same physical properties, the new branch corresponds to the so-called anomalous solution. Based on symmetry properties we could easily infer—using our results on the asymmetric phase diagram—what the new solution should look like.

The parity-breaking bifurcation is now well understood both numerically and analytically. Inspired by our work on parity breaking, we have built up an analytic theory for the birth of the anomalous branch. We found that the corresponding bifurcation takes place at a wavelength which is approximately double that of the minimum undercooling. This branch has a higher undercooling than the global parity-breaking solution. Our analytic theory has the important advantage that it is pedestrian in its spirit but captures the essential features.

We have developed for the (generic) asymmetric phase diagram a simple phenomenological picture based on Landau theory to argue that the new branch is less stable than the old one. This result is consistent with the belief that systems often select solutions with the smallest undercooling; indeed, the new branch has a higher undercooling, and the minimum undercooling principle is therefore in favor of the old branch. It is not our intention to pretend that the minimum undercooling principle should be absolutely operative, but simply that its prediction seems often to be in agreement with observations. It is very important to note, however, that despite the fact that the tilted pattern has a higher undercooling, its experimental observation as an extended state, during a long time (basically during the full time of the experiment), is now a well-established fact [27].

The experiment in question was based on the (simple) experimental protocol we had suggested, namely a sudden jump of the growth speed by a factor of about 4. We believe that our suggestion for the experimental protocol, consisting of “quenching” the system in a controlled way,

should give access not only to the new tilted state but more generally to the existence of a discrete set of solutions, which we brought out by solving fully the boundary integral equation.

Experiments on eutectic systems, which have already been impressively successful [27], are, in our opinion, of a unique type in the pattern formation of crystal growth, having direct access to a “countable” set of solutions, even those which can be presumed unstable, at least when one has in mind the minimum undercooling principle. A major advantage of this system lies in the slow phase diffusion process, which allows one to impose easily temporarily various wavelengths. This situation, where part of the theory has already been confirmed by experiments, contrasts strongly with that of velocity selection in free dendritic growth, where there has not been to date and, to our knowledge, a crucial experimental test, a fact which still sustains a controversy about the theory.

ACKNOWLEDGMENTS

K.K., C.M., and A.V. benefited from financial support under NATO Grant No. CRG.920541.

APPENDIX: DETERMINATION OF THE PARITY OF F

We would like to check that F is antisymmetric with respect to y_0 . So we consider the quantity $F(-y_0)$, which is given by

$$F(-y_0) = \int_0^{\lambda/2} \frac{f(x, -y_0)}{\sqrt{1+f^2(x, -y_0)}} dx, \quad (\text{A1})$$

with

$$f(x, -y_0) = \sin\theta + \int_0^x \frac{u(X, -y_0) - \Delta(-y_0)}{d_0} dX. \quad (\text{A2})$$

Let $Y = \lambda/2 - X$ in the expression of $f(x, -y_0)$. We

obtain then

$$f(x, -y_0) = \sin\theta - \int_{\lambda/2}^{\lambda/2-x} \frac{u(Y, y_0) - \Delta(y_0)}{d_0} dY, \quad (\text{A3})$$

where we have exploited the symmetry property of the coefficients D_n (which enter the diffusion field definition). Namely, due to that symmetry we have $u(X, -y_0) = u(Y, y_0)$ and $\Delta(-y_0) = \Delta(y_0)$.

The strategy now is to split the integral in (A3) into two parts in the following manner:

$$f(x, -y_0) = \sin\theta - \int_{\lambda/2}^0 \frac{u(Y, y_0) - \Delta(y_0)}{d_0} dY - \int_0^{\lambda/2-x} \frac{u(Y, y_0) - \Delta(y_0)}{d_0} dY. \quad (\text{A4})$$

The first integral can easily be evaluated by using the Gibbs-Thomson relation for the α phase ($d_0\kappa = u - \Delta$). The result is $2 \sin\theta$, so that (A4) takes the following form:

$$f(x, -y_0) = -\sin\theta - \int_0^{\lambda/2-x} \frac{u(Y, y_0) - \Delta(y_0)}{d_0} dY = -f(\lambda/2 - x, y_0). \quad (\text{A5})$$

It suffices now to insert this relation into Eq. (A1) and to make the last change of variable $X = \lambda/2 - x$ to obtain the desired equality:

$$F(-y_0) = - \int_0^{\lambda/2} \frac{f(\lambda/2 - x, y_0)}{\sqrt{1+f^2(\lambda/2 - x, y_0)}} dx = - \int_0^{\lambda/2} \frac{f(X, y_0)}{\sqrt{1+f^2(X, y_0)}} dX = -F(y_0). \quad (\text{A6})$$

*Also at Groupe de Physique des Solides, Universit s Paris 7 et 6, 2 Place Jussieu, 75005 Paris, France.

†Present address: Laboratoire de Physique de l'E.N.S. de Lyon, 46 All e d'Italie, 69000 Lyon, France. Permanent address: I. P. Bardin Institute for Ferrous Metals, Moscow 107005, Russia.

- [1] K. A. Jackson and J. D. Hunt, *Trans. Metall. Soc. AIME* **236**, 1129 (1966).
- [2] C. Zener, *Trans. Metall. Soc. AIME* **167**, 550 (1946).
- [3] G. E. Nash, *J. Cryst. Growth* **38**, 155 (1977).
- [4] R. W. Series, J. D. Hunt, and K. A. Jackson, *J. Cryst. Growth* **40**, 221 (1977).
- [5] R. Trivedi, P. Magnin, and W. Kurz, *Acta. Metall.* **35**, 971 (1987).
- [6] M. B. Geilikman and D. E. Temkin, *Kristallografiya* **29**, 643 (1984) [*Sov. Phys. Crystallogr.* **29**, 381 (1984)].
- [7] D. E. Temkin, *Kristallografiya* **30**, 1055 (1985) [*Sov. Phys. Crystallogr.* **30**, 613 (1985)].
- [8] K. Brattkus, B. Caroli, C. Caroli, and B. Roulet, *J. Phys.*

(France) **51**, 1847 (1990).

[9] C. Misbah (unpublished).

[10] J. S. Langer, *Phys. Rev. Lett.* **44**, 1023 (1980).

[11] V. Datye and J. S. Langer, *Phys. Rev. B* **24**, 4155 (1981).

[12] B. Caroli, C. Caroli, and B. Roulet, *J. Phys. (France)* **51**, 1865 (1990).

[13] K. Kassner and C. Misbah (unpublished).

[14] K. Brattkus and C. Misbah, *Phys. Rev. Lett.* **64**, 1935 (1990).

[15] A. Karma, *Phys. Rev. Lett.* **59**, 71 (1987).

[16] C. Faivre, S. de Cheveign , C. Guthmann, and P. Kurowski, *Europhys. Lett.* **9**, 779 (1989).

[17] K. Kassner and C. Misbah, *Phys. Rev. Lett.* **65**, 1458 (1990); **66**, 522(E) (1991).

[18] K. Kassner and C. Misbah, *Phys. Rev. Lett.* **66**, 445 (1991).

[19] K. Kassner and C. Misbah, *Phys. Rev. A* **44**, 6513 (1991).

[20] K. Kassner and C. Misbah, *Phys. Rev. A* **44**, 6533 (1991).

[21] K. Kassner and C. Misbah, *J. Phys. A* **25**, 3213 (1992).

- [22] C. Misbah and D. E. Temkin, *Phys. Rev. A* **46**, R4497 (1992).
- [23] Alexandre Valance, Chaouqi Misbah, Dmitrii Temkin, and Klaus Kassner (unpublished).
- [24] A. J. Simon, J. Bechhoefer, and A. Libchaber, *Phys. Rev. Lett.* **63**, 2574 (1988).
- [25] R. Racek, Ph.D. thesis, Thèse d'Université, Nancy I, 1973 (unpublished).
- [26] P. Couillet, R. Goldstein, and G. H. Gunaratne, *Phys. Rev. Lett.* **63**, 2574 (1989).
- [27] G. Faivre and J. Mergy, *Phys. Rev. A* **45**, 7320 (1992).
- [28] J.-M. Liu, *Scripta Metall. Mater.* **26**, 179 (1992).
- [29] B. Caroli, C. Caroli, and S. Fauve, *J. Phys. I (France)* **2**, 281 (1992).
- [30] K. Kassner and C. Misbah, *Phys. Rev. A* **45**, 7372 (1992).
- [31] G. Faivre and J. Mergy, *Phys. Rev. A* **46**, 963 (1992).
- [32] M. R. E. Proctor and C. A. Jones, *J. Fluid Mech.* **188**, 301 (1988).
- [33] H. Levine and W. J. Rappel, *Phys. Rev. A* **42**, 7475 (1990).
- [34] M. Rabaud, S. Michalland, and Y. Couder, *Phys. Rev. Lett.* **64**, 184 (1990).
- [35] P. Oswald, *J. Phys. II (France)* **1**, 571 (1991).
- [36] S. de Cheveigné and C. Guthmann, *J. Phys. I (France)* **2**, 193 (1992).
- [37] Lengths are measured in multiples of l_T and times in multiples of $\tau \equiv l_T^2/D$. As an example for the mapping to physical units, we consider typical values for the parameters in directional solidification of $\text{CBr}_4\text{-C}_2\text{Cl}_6$ [41]: $\Delta c = 9.7$ mol %, $\Delta T_\alpha \equiv m_\alpha \Delta c = 8$ K, $G = 85$ K/cm, and $D = 5 \times 10^{-6}$ cm²/s. Therefore, $l_T^g = 0.094$ cm and the time unit is $\tau = 1771.6$ s. The other quantities are calculated as $\lambda_{\min} = 10.4$ μm , $V = 2.1$ $\mu\text{m/s}$, and $d_0^{g/\beta} = 9.5$ nm.
- [38] Rong-Fu Xiao, J. Iwan, D. Alexander, and Franz Rosenberger (unpublished).
- [39] It has retained symmetry under a simultaneous exchange of the two phases and a reflection on an α - β lamella boundary.
- [40] P. Oswald (private communication).
- [41] B. Caroli, C. Caroli, G. Faivre, and J. Mergy, *J. Cryst. Growth* **118**, 135 (1992).